CODED 64-CAP ADSL IN AN IMPULSE-NOISE ENVIRONMENT — SIMULATION RESULTS —

Werner Henkel
Research Center of Deutsche Telekom
D-64276 Darmstadt, Germany
EMAIL: henkel@fz.telekom.de

Hong Y. Chung
AT&T Bell Laboratories
Holmdel, NJ 07733, USA
EMAIL: hychung@attmail.com

Abstract — This paper describes performance results of E1-ADSL (2.048 Mb/s asymmetrical digital subscriber line) transmission based on **C**arrierless **A**mplitude / **P**hase Modulation (CAP) in an impulse-noise environment. Various coding schemes for error protection are investigated. Code options are Reed Solomon code with interleaving, array code and trellis coding, or interleaved trellis coding.

The simulation results are based on real measured impulses from an impulse-noise measurement campaign carried out by German Telekom. The inter-arrival times between impulses were either assumed to be constant (worst-case scenario) or were delivered from a distinctive stochastic generator with an inter-arrival time density according to a model also derived in the German campaign. It was found that RS codes, even with a quite small error-correcting capability, achieved acceptable error performances. Array codes can also be a low-complexity alternative. Trellis coding alone, as expected, was not very effective against the impulse noise.

I. INTRODUCTION

The asymmetrical digital subscriber line (ADSL) [1, 2] provides very high bit-rate video services to residential customers over unshielded twisted pairs. The ADSL operates at a data rate of 2.048 Mb/s for E1 rate (1.544 Mb/s for primary T1 rate) over subscriber loops from the central office (CO) to the customer, and a lower rate control channel is provided for the other direction. Since the copper medium used for ADSL services suffers a high propagation loss and a possible cross-talk (NEXT) from other types of services as the transmission length and the signal bandwidth increase, the ADSL requires a bandwidth-efficient modulation scheme that can reliably carry the information. Carrierless amplitude/phase (CAP) modulation [3], which is a variant of quadrature amplitude modulation (QAM), is well suited for this type of application, because of its inherent bandwidth efficiency and the compatibility with error-correcting codes. The ADSL, however, also suffers from impulse noise. Impulse noise caused by relay reopenings and from various other sources [4] can have a significant impact on compressed video signals in the ADSL. Although it is well known that the trellis-coded modulation (TCM) [5] used in conjunction with CAP or QAM can provide 3-5 dB coding gains in an additive white Gaussian noise (AWGN) environment where random errors are dominant, it may not be able to provide the same performance in an environment where bursty or colored noise such as NEXT are dominant. Bursty errors are usually generated by impulse noise and can also result from NEXT affecting consecutive symbols in the Viterbi decoder, because such a decoder relies on the past history of the symbol sequence. Thus, a coding scheme is required for the ADSL that is robust against impulse noise in order to minimize its impact on the compressed video signals. Impulses that are used in this study were taken from one site of the German survey where the impulse noise was considered to have quite typical statistical properties (see, [8, 10, 11, 12]).

It is the main purpose of this paper to present performance results of coding schemes using several component codes such as Reed-Solomon (RS) codes, array codes, and trellis codes to mitigate the effects of impulse noise. RS codes are well suited for the ADSL application, because they are known to be very effective for correcting multiple bursts of errors [6]. Although array codes are not originally designed for correcting a burst of errors, we also investigate array codes with diagonal readout whose symbols are comprised of multiple bits [9]. These codes turned out to be able to provide a good error-correcting capability with a low decoding complexity at the receiving end as compared to RS codes.

The remainder of the paper is organized as follows. Section 2 gives an overview of the considered coding schemes that were applied to 64-CAP. Section 3 provides error-performance results in impulse noise for the various configurations of coding schemes obtained by computer simulation. First, a constant inter-arrival time is assumed, whereas Section 4 presents results when using stochastic inter-arrival times supplied by a dedicated generator that follows a model of the real inter-arrival time statistics. Finally, discussions and a summary are given in Section 5.

II. SYSTEM DESCRIPTION AND SIMULATED SCHEMES

In this section, we present block diagrams for the coded schemes that are simulated in this study. There are several coding schemes we consider for an impulse-dominated environment. These are either RS-coded, trellis-coded, or both RS- and trellis-coded CAP schemes. Array codes will also be used. The performance of the uncoded scheme that transmits the same data rate as the coded schemes will be used as a basis for comparison throughout the paper. Some coded schemes will have interleaving to further distribute the errors before the decoding. However, it should be noted that the interleaving increases the overall transmission delay and should be designed to meet the delay specifications set by the customers.

Trellis code only

We first start with a scheme that uses trellis code only, which is shown in Fig. 1a. The trellis code used here is a 2-dimensional 8-state trellis code [7]. As shown in Fig. 1a, the encoder encodes 5 information bits into 6 bits, which in turn are mapped on to

0-7803-2509-5/95 US$4.00

the 64-CAP (8×8) square signal constellation.[1]

As mentioned before, the TCM in general is very effective in AWGN, providing a significantly larger noise margin over an uncoded counterpart. However, in an impulse-noise environment, because of the nature of the maximum-likelihood sequence estimation algorithm used in the decoding of trellis-coded symbols (Viterbi algorithm), it is not very effective when several consecutive received symbols are corrupted by impulse noise. We also simulated an interleaved trellis code, which utilizes more than one encoder and decoder pair in a time-multiplexed fashion. The effect of using this type of scheme is to distribute the errors caused by an impulse into several decoders so that they could be corrected by the decoders. This will, however, increase the decoding delay by a factor of ν, where ν is the number of encoder/decoder pairs used in the scheme.

Reed-Solomon code only

Figure 1b shows a block diagram for an RS-coded 64-CAP scheme. The (n, k) RS codes used in this study are (135, 131) $t = 2$, (135, 129) $t = 3$, and (135, 127) $t = 4$ with symbols from Galois field $GF(2^8)$, where t denotes the symbol error-correcting capability of the code. It should be noted that, for (n, k) RS-coded schemes, the signal bandwidth is increased by a factor of n/k compared to the uncoded case. The n and k parameters were chosen to optimize signal framing and the bandwidth expansion.

Concatenated code

A block diagram for the concatenated coded scheme that uses both the RS codes and the trellis code is shown in Fig. 1c. The main idea of concatenating two or more codes together is to use additional decoders to further correct the errors after the first decoder, if the output from the first decoder forms a correctable pattern for the additional decoders. Due to the constraints on delay and complexity, concatenated codes usually use only two codes, namely, inner code and outer code. The scheme can also use a symbol interleaving between the inner and outer codes to distribute the errors at the output of the inner decoder at the receiver. This can help the outer decoder to correct errors that are still remaining after the inner decoder. However, the interleaving depth, which defines the degree of interleaving in symbols, should be determined carefully not to affect the performance of the outer decoder. It will be shown later that a larger interleaving depth does not necessarily provide a better performance and can have an adverse effect on the outer decoder. Finally, array codes are also simulated by replacing the RS codes shown in the figures.

III. SIMULATION RESULTS BASED ON REAL MEASURED IMPULSES AND CONSTANT INTER-ARRIVAL TIMES (A WORST-CASE STUDY)

[1]Although 64-CAP is used for all coded and uncoded schemes presented in this paper, signal constellations of different sizes can also be used. Changing the number of signal points in the constellation, however, will change the system bandwidth and, consequently, will slightly affect the overall performance.

This section describes first results obtained when following a data-bank approach. Transmission of a 64-CAP signal was studied under impulse noise which was taken from one location of the German Telekom survey where the statistics were quite typical. A few impulses are shown in Fig. 2.

51,200 impulse events were stored in compressed form on a magneto-optical disk or a hard disk. Their sample interval is $1/10.24$ MHz $= 0.0977$ μs. During the simulation, the real measured data were read from the disk. The amplitudes of the impulses were not changed. The gap between two impulses was inserted as a sequence of zeros in such a way that the inter-arrival times of the simulated impulse noise are either constant (500 CAP symbols ≈ 1.4 ms) or, as described in the next section, distributed according to the modeling density for the inter-arrival times. The time span for the constant inter-arrival time simulations is located right after a minimum at the beginning of the real inter-arrival time distribution (see, [8, 10, 11, 12]). Below this minimum, measured inter-arrival times mostly belonged to trigger events inside the same impulse. Hence, the chosen constant inter-arrival time is suited for a worst-case study.

After the data-bank access, a sampling-rate conversion has to be applied in order to adapt the sampling rate to the processing rate (chosen to be the 4-fold symbol rate) of the simulated configuration.

Two different loops were considered: a standard loop of 12 kft, 24 gauge and a quite long one of 4.25 km and 0.4 mm diameter. The totally uncoded error-burst length statistics are presented in figures 3a and 3b, respectively. An error burst is defined to be separated by at least 10 error-free CAP symbols.

Of course, both figures show similarities to the original impulse-length distribution in [11], which is approximately described by a sum of two log-normal densities. The error length distribution has significant components at up to 30 CAP symbols for the short loop and about 80 symbols in the case of the long one. The corresponding symbol-error rates are $1.2 \cdot 10^{-3}$ and $3.3 \cdot 10^{-2}$, respectively. The uncoded error rate for the long loop is quite poor. Hence, no significant coding gains are expected from *any* error-correcting code. The following coding schemes were considered:

- 8-state trellis code (Wei)
- interleaved trellis coding (interleaving depth = 16)
- Reed-Solomon codes of length 135 symbols over GF(2^8) with an error correcting capability of $t = 2, 3, 4$ together with interleaving of depths 18, 24, and 36
- array codes as burst error correcting codes with n_1 rows and $n_2 = 2n_1 - 3$ columns and a maximum correctable single burst of length $n_1 - 1$

The Reed-Solomon (RS) parameters are not optimized for the chosen impulse-noise environment, especially not for the fixed inter-arrival time. The parameters are the ones that were discussed in the corresponding standardization groups (ANSI). Nevertheless, at least the array size of the array code was chosen such that at most one impulse event occurs within an array. Ignoring the quite short inter-arrival time and regarding the length

distribution in Fig. 3a, the first set of RS parameters seems not to be unrealistic. With $t = 2$ and an interleaving depth of $D = 18$, a burst-error correcting capability of $t \cdot D = 36$ is achieved which corresponds to $36 \cdot 8/6 = 48$ CAP symbols. This should be enough for the maximum burst lengths of the short loop.

We shall now consider the application of coded modulation. As an example, we applied an 8-state two-dimensional scheme. This improved the symbol-error rate slightly in the case of the short loop ($8.36 \cdot 10^{-4}$), but was quite destructive with the long loop (0.56). Trellis coding together with Viterbi decoding can, of course, not handle severe bursty noise. The error-length distribution in Fig. 3c (short loop) shows similarities to the uncoded case except that short error events are reduced. Even an interleaved trellis coding with an interleaving depth of up to 16 is not very effective. The symbol-error rate is further slightly reduced to $5.71 \cdot 10^{-4}$ (short loop). The error-length distribution is shown in Fig. 3d. The relatively strong single-error component is due to the underlying burst definition: a new error burst starts after at least 10 error-free symbols. In the sequel, only results for the short loop are given, unless otherwise stated.

A very effective burst correction is expected and obtained with RS codes. Without any additional trellis coding and with an interleaving depth of 18 symbols (8 bits), we achieved symbol-(8 bits)-error rates of $1.26 \cdot 10^{-4}, 2.06 \cdot 10^{-5}$, and $2.10 \cdot 10^{-6}$ (bit-error rate $= 8.17 \cdot 10^{-7}$) for $t = 2$, 3, and 4, respectively. The length statistic for $t = 2$ is given in Fig. 3e. The statistics for $t = 3$ and $t = 4$ look very similar. With additional trellis coding, the error rates are further reduced to $5.84 \cdot 10^{-5}$ ($t = 2$), $4.91 \cdot 10^{-6}$ ($t = 3$), and actually no error for $t = 4$.

With the long loop and $t = 2$, the symbol-error rate was about $3.9 \cdot 10^{-2}$ for interleaving depths between 18 and 36. Hence, effectively no coding gain is obtained with the long loop. Even for the short loop, an increase of the interleaving depth does not improve the error rate significantly. For $t = 2$ and no additional trellis coding, the symbol error rates are $1.26 \cdot 10^{-4}, 9.63 \cdot 10^{-5}$, and $7.46 \cdot 10^{-5}$ for $D = 18$, $D = 24$, and $D = 36$, respectively. As already mentioned, the interleaving depth of $D = 18$ together with $t = 2$ is reasonable as far as the uncoded symbol-error length distribution is concerned. On the other hand, a further increase in the interleaving depth means that more impulse events fall into one interleaver matrix, thereby possibly exceeding the error-correcting capability of the RS code.

As an alternative to RS codes, array codes with a diagonal readout were investigated. Their advantage is their relatively low decoding complexity due to the fact that the component codes are simple parity-check codes. Their disadvantage is that they are pure (single) burst correcting which means that additional random errors can easily lead to an uncorrectable error pattern. Furthermore, the probability of wrong correction is not as small as for RS codes. However, if impulse noise is dominant, array codes may be a worthwhile alternative.

Array codes are described by three parameters: n_1, the number of rows, n_2, the number of columns, and s, the shift between the output diagonals. We only considered $s = 1$. One can show (see, [13, 14] and [9]) that such array codes with $n_2 \geq 2n_1 - 3$ are capable of correcting cyclic bursts of at most $n_1 - 1$ bits or symbols. The term 'symbol' stands for the components of non-binary array codes; where each array component consists of a vector of binary digits (or of other group elements). The array code is made up from parity checks in rows and columns. In the case of binary component vectors, the parity checks are computed separately for every component. An exemplary array with the readout cycle and the location of the parity checks is shown subsequently.

0	6	12	18	24	30	36	42	48
49	1	7	13	19	25	31	37	43
44	50	2	8	14	20	26	32	38
39	45	51	3	9	15	21	27	33
34	40	46	52	4	10	16	22	28
29	35	41	47	53	5	11	17	23

(1)

The performance of array codes can be further improved by reducing the coding/decoding delay. A proposal to decrease the coder-delay has been made in [9], leading to an overall reduction by about 35%. The scheme uses three different filling modes together with a prefilled area of the array. The filling cycle for (1) is given as follows:

0	5	9	17	19	*	*	12	@
24	1	6	10	18	*	*	13	@
25	29	2	7	11	*	*	14	@
26	27	28	3	8	*	*	15	@
20	21	22	23	4	*	*	16	@
@	@	@	@	@	@	@	@	–

(2)

*: prefilled positions, @: parity symbols, –: parity-of-parities (left empty)

The decoding algorithm was taken from [13, 14] and consists in principle of a search for the largest consecutive cyclic range of columns whose parity checks are not violated. The burst starts right after it. The exact burst location in a cyclically continued diagonal is determined by jointly considering the parity violations in the rows, too. Thus, column and row parity violations represent the actual error pattern.

Two exemplary simulation runs were carried out. In one case, the array size was adapted to the inter-arrival time with $n_1 = 13$ and $n_2 = 2n_1 - 3 = 23$, whereas the parameters in the second run were $n_1 = 100$ and $n_2 = 2n_1 - 3 = 197$. The symbols were chosen from GF(2^8) as for the RS codes. Together with included trellis coding, symbol error rates of $8.85 \cdot 10^{-5}$ and $1.01 \cdot 10^{-3}$, respectively, were achieved. The second result reveals the drawback of single-burst correcting codes when multiple bursts occur within one array. Nevertheless, the first result is comparable to an RS code with $t = 2$ and $D = 18$, but with lower rate ($1 - \frac{13+23-1}{13 \cdot 23} = 0.883$). With real inter-arrival times, the array size may be further increased, thereby increasing the rate, too.

An overview over all simulation results is given in Table 1.

IV. SIMULATION RESULTS WITH STOCHASTIC INTER-ARRIVAL TIMES

When stochastic inter-arrival times according to the density

$$f_d(x) = \frac{10^{a_1}}{\ln(10)} x^{a_4 - 1} 10^{-\frac{a_4}{\ln(a_2)} a_2^{(\log_{10}(x) - a_3)}} \tag{3}$$

(see [8, 10, 11, 12]; $a_2 = 2.22$, $a_3 = 5.15$, $a_4 = 1.26$, $x = t/100$ ns) are used, more realistic results for the error probabilities are obtained. Hereto, a specially developed generator for the inter-arrival times was used (see, [8, 11, 12]). Although some time-optimizing programming techniques have been applied, the run time for simulations is quite high.

First, by using realistic inter-arrival times, the totally uncoded symbol-(6 bits)-error rate is reduced significantly to $2.8 \cdot 10^{-5}$ for the short loop and $7.82 \cdot 10^{-4}$ for the long loop (Table 2). An RS code with $t = 2$ reduces these to $1.14 \cdot 10^{-7}$ and $2.98 \cdot 10^{-4}$ (8-bit symbols), respectively. We conclude that such a simple RS code yields acceptable results for the short loop, whereas the protection for the long loop is not sufficient. A $t = 4$ code further decreased the symbol-error rate to $3.93 \cdot 10^{-5}$ in the case of the long loop. An increase in the interleaving depth then leads to a reasonable error performance of $4.92 \cdot 10^{-6}$, because with real inter-arrival times, an increase of the interleaving depth is not as critical as in the case of the previous section where a rather short inter-arrival time resulted in multiple bursts within the interleaver matrix.

These results show that even with quite weak RS codes, an acceptable error protection in an impulse-noise environment can be guaranteed. Array codes achieve a symbol-error rate of $3.86 \cdot 10^{-6}$ for the short loop with $n_1 = 13$. A further increase of the array size is disadvantageous due to the restriction of the error-correcting capability to only one burst.

	without trellis code	with trellis code	with interleaved trellis code
short loop			
no outer code	$1.18 \cdot 10^{-3}$	$8.36 \cdot 10^{-4}$	$5.71 \cdot 10^{-4}$
RS, $t = 2$, $D = 18$	$1.26 \cdot 10^{-4}$	$5.84 \cdot 10^{-5}$	$7.57 \cdot 10^{-5}$
RS, $t = 3$, $D = 18$	$2.06 \cdot 10^{-5}$	$4.91 \cdot 10^{-6}$	
RS, $t = 4$, $D = 18$	$2.10 \cdot 10^{-6}$	no error	$1.40 \cdot 10^{-6}$
RS, $t = 2$, $D = 24$	$9.63 \cdot 10^{-5}$		
RS, $t = 2$, $D = 36$	$7.46 \cdot 10^{-5}$		
ARRAY, $n_1 = 13$		$8.85 \cdot 10^{-5}$	
ARRAY, $n_1 = 100$		$1.01 \cdot 10^{-3}$	
long loop			
no outer code	$3.30 \cdot 10^{-2}$	$5.6 \cdot 10^{-1}$	$4.5 \cdot 10^{-2}$
RS, $t = 2$, $D = 18$	$3.85 \cdot 10^{-2}$		
RS, $t = 2$, $D = 36$	$3.88 \cdot 10^{-2}$		

Table 1: Overview over the simulation results with *constant* inter-arrival time

V. SUMMARY AND CONCLUSIONS

The error performance results of various coding schemes for the CAP (carrierless amplitude/phase modulation) -based ADSL (asymmetrical digital subscriber line) under impulse-noise disturbance were presented. The investigations were performed using the data of an impulse-noise measurement campaign, carried out by German Telekom.

The simulations were based on a data-bank approach, selecting stored impulse events from one location of the whole measurement campaign. First, a constant quite short inter-arrival time was chosen to obtain some worst case results. In a second phase, real inter-arrival times were generated by a specially developed generator. The following coding schemes were studied: 8-state trellis code, interleaved trellis coding, Reed-Solomon codes with symbol interleaver, and array codes with diagonal readout. It was found that relatively weak Reed-Solomon codes with a correcting capability between 2 and 4 symbols together with an interleaving depth between 18 and 36 yielded acceptable error performances on two exemplary loops (12 kft, 24 gauge and 4.25 km, 0.4 mm). A Reed-Solomon (135, 131) t=2 code with an interleaving depth of 18 codeword symbols provided an acceptable error performance while the codes with $t > 2$ yielded no errors for the same interleaving depth. It was also found that increasing the interleaving depth above 18 codewords did not improve the performance for short inter-arrival times. The performance with 24- and 36-symbol interleaving actually was a slightly deteriorated. This is probably because the change in the data sequence in the longer interleaving cases produced long error bursts. Trellis coding alone was not effective against impulse noise. Its performance was only slightly better than that of the uncoded scheme for the short loop, but was almost disastrous for the long one. Although the performance of array codes was not as good as that of the Reed-Solomon codes, those codes can be an alternative in an impulse-noise environment where a very low decoding complexity is required for a modest error performance.

	without trellis code	with trellis code
short loop		
no outer code	$2.80 \cdot 10^{-5}$	$1.6 \cdot 10^{-5}$
RS, $t = 2$, $D = 18$	$1.14 \cdot 10^{-7}$	$5.73 \cdot 10^{-9}$
RS, $t = 3$, $D = 18$	0	0
RS, $t = 4$, $D = 18$	0	0
RS, $t = 2$, $D = 24$	$4.97 \cdot 10^{-8}$	$6.65 \cdot 10^{-8}$
RS, $t = 2$, $D = 36$	$3.72 \cdot 10^{-9}$	0
ARRAY, $n_1 = 13$	$3.86 \cdot 10^{-6}$	$2.71 \cdot 10^{-6}$
ARRAY, $n_1 = 23$	$4.50 \cdot 10^{-6}$	$2.07 \cdot 10^{-6}$
ARRAY, $n_1 = 33$	$5.53 \cdot 10^{-6}$	$2.16 \cdot 10^{-6}$
long loop		
no outer code	$7.82 \cdot 10^{-4}$	
RS, $t = 2$, $D = 18$	$2.98 \cdot 10^{-4}$	
RS, $t = 4$, $D = 18$	$3.93 \cdot 10^{-5}$	
RS, $t = 4$, $D = 36$	$4.92 \cdot 10^{-6}$	

Table 2: Overview over the simulation results with *stochastic* inter-arrival time

References

[1] **Sistanizadeh, K.:** Ad Hoc Meeting Report on ADSL Loop Reach, Channel Rates, & PSD, *T1E1.4 Ad Hoc Meeting Contribution T1E1.4/93-150*, May 11, 1993.

[2] **Sorbara, M., Schreibmaier, R.A.:** Carrierless AM/PM (CAP) Asymmetrical Digital Subscriber Line (ADSL) Transceiver, *CAP ADSL Transceiver System Requirements*, AT&T, Sept. 1993.

[3] **Sorbara, M., Werner, J.-J., Zervos, N.:** Carrierless AM/PM, *HDSL contribution to T1E1.4*, T1E1.4/90-154, Sept. 1990.

[4] **Werner, J.-J.:**, Impulse noise in the loop plant, *Proceedings of ICC'90*, Atlanta, GA, April 1990.

[5] **Ungerboeck, G.:**, Channel coding with multi-level/phase signals, *IEEE Trans. Info. Th.*, Vol. IT-28, No. 1, pp. 55-67, Jan. 1982.

[6] **Lin and Costello:**, *Error Control Coding: Fundamentals and Applications*, Prentice Hall, 1983.

[7] **CCITT Study Group XVII:** Recommendation V.32 for a family of 2-wire duplex modems operating at data signalling rate of up to 9600 bps for use on the general switched telephone network and on leased telephone-type circuits, Document AP VIII-43-E, May 1984.

[8] **Henkel, W., Kessler, T., Chung, H.Y.:** A Wide-Band Impulse-Noise Survey on Subscriber Lines and Inter-Office Trunks - Modeling and Simulation -, *Globecom/CTMC '95*, Singapore, Nov. 13-17, 1995.

[9] **Henkel, W., Chung, H.Y.:** A New Filling Procedure to Reduce the Delay of Burst-Error Correcting Array Codes, *Electronics Letters*, Vol. 30, No. 6, March 17, 1994, pp. 465-466.

[10] **Henkel, W., Kessler, T.:** Statistical Description and Modeling of Impulsive Noise on the German Telephone Network, *Electronics Letters*, Vol. 30, No. 12, June 9, 1994, pp. 935-936.

[11] **Henkel, W., Kessler, T.:** A Wideband Impulsive Noise Survey in the German Telephone Network: Statistical Description and Modeling, *AEÜ*, Vol. 48, No. 6, pp. 277-288, Nov./Dec. 1994.

[12] **Henkel, W., Kessler, T., Chung, H.Y.:** Coded 64-CAP ADSL in an impulse-noise environment — modeling of impulse noise and first simulation results —, *IEEE J. Sel. Ar. Comm.*, Dec. 1995.

[13] **van Tilborg, H.C.A.:** An Overview of Recent Results in the Theory of Burst-Correcting Codes, *Springer Lecture Notes in Computer Science 388*, pp. 164-184, 1988.

[14] **Blaum, M., Farrell, P.G., van Tilborg, H.C.A.:** A Class of Burst Error-Correcting Array Codes, *IEEE Trans. on Information Theory*, Vol. IT-32, No. 6, pp. 836-839, Nov. 1986.

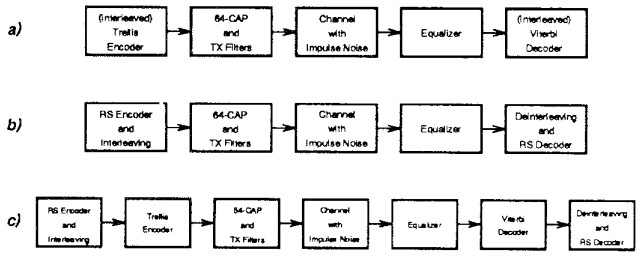

Figure 1: Simulated coding schemes

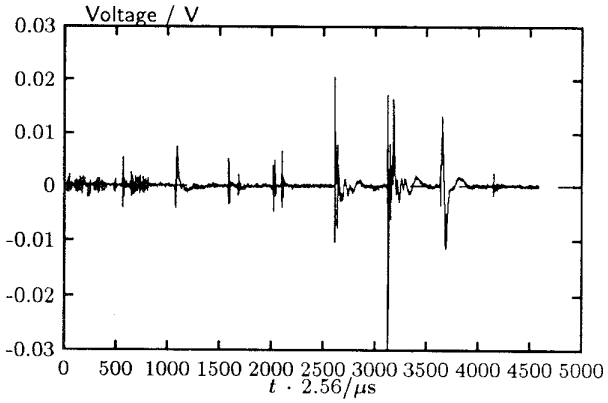

Figure 2: Some sample impulses (location: Mayence)

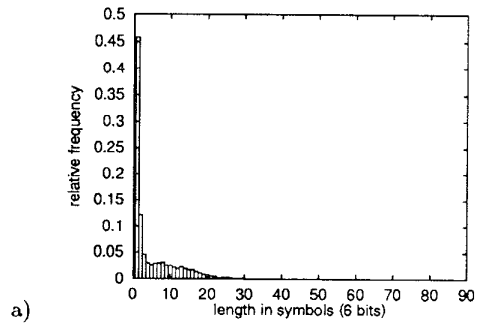

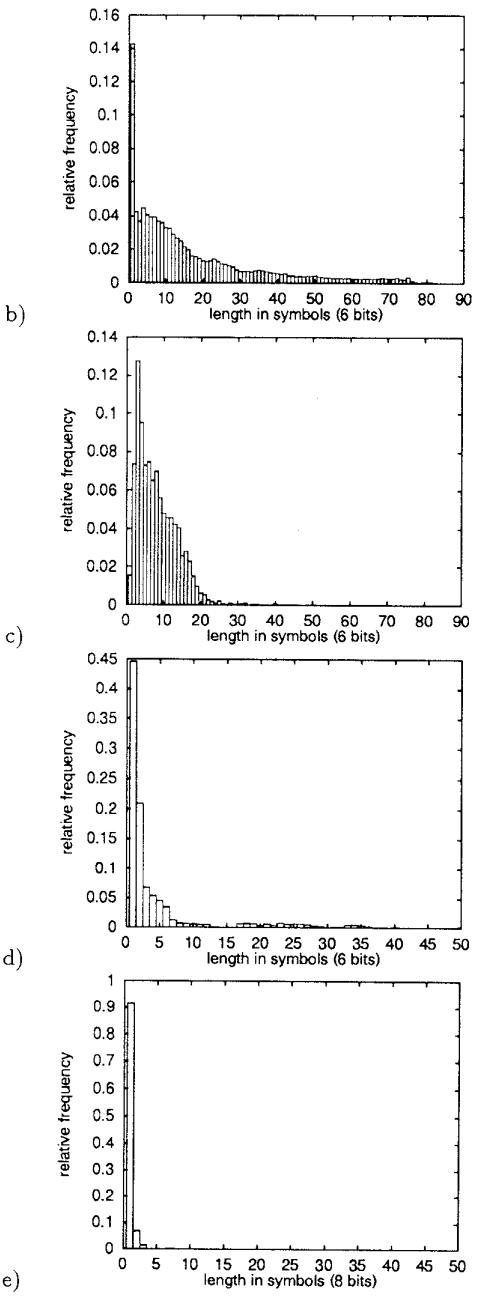

Figure 3: Symbol-error length frequency distribution
a) without coding (12 kft, 24 gauge)
b) without coding (4.25 km, 0.4 mm)
c) with included 2-dimensional trellis coding (12 kft, 24 gauge)
d) with included interleaved trellis coding (interleaving depth: 16; 12 kft, 24 gauge)
e) with included Reed-Solomon code ($t = 2$, $D = 18$; 12 kft, 24 gauge)